A Letters Journal Exploring the Frontiers of Physics

February 2010

EPL, **89** (2010) 38005
doi: 10.1209/0295-5075/89/38005

www.epljournal.org

Jamming of polydisperse hard spheres: The effect of kinetic arrest

M. Hermes and M. Dijkstra

Soft Condensed Matter group, Debye Institute for Nanomaterials Science, Utrecht University Princetonplein 5, 3584 CC Utrecht, The Netherlands, EU

received 20 July 2009; accepted in final form 14 January 2010
published online 16 February 2010

PACS 82.70.Dd – Colloids
PACS 61.43.Fs – Glasses
PACS 64.70.Q- – Theory and modeling of the glass transition

Abstract – We study jammed configurations of polydisperse colloidal hard spheres with a well-defined temperature (constant kinetic energy) as a function of compression speed and size polydispersity. To this end, we employ event-driven molecular-dynamics simulations at fixed temperature, using an algorithm that strictly prohibits particle overlaps. We find a strong dependence of the jamming density on the compression rate that cannot be explained by crystallization. Additionally, we find that during the compression, the pressure follows the metastable liquid branch until the system gets kinetically arrested. Our results show that further compression yields jammed configurations that can be regarded as the infinite-pressure limit of glassy states and that different glasses can jam at different jamming densities depending on the compression rate. We present accurate data for the jamming density as a function of compression rate and size polydispersity.

Colloidal hard spheres have proven their value as a model system for the study of liquids, glasses, crystals and powders. In 2005, Hales proved Kepler's conjecture that the densest packing of N identical hard spheres in a volume V is achieved by the stacking of close-packed hexagonal planes yielding a packing fraction $\phi = \pi\sigma^3 N/6V \approx 0.74$ [1]. When a colloidal system is compressed slowly it indeed forms this close-packed crystal phase [2]. However, when a system of hard spherical colloids is compressed quickly it does not reach this maximum density and it forms a jammed configuration at a lower density as further compression leads to particle overlaps or deformation [3]. Jamming phenomena are generic since atomic, colloidal and granular systems can all be jammed in a state out of equilibrium by quickly cooling, compressing or unloading [4]. In experiments on colloidal systems, which are inherently polydisperse in size, the packing fraction is often determined by centrifuging the sample and equating the packing fraction of the sediment [5] to the jamming or random-close-packing density $\phi_{\rm rcp}$, and hence requires an accurate value of $\phi_{\rm rcp}$.

Many authors speculate that $\phi_{\rm rcp} \sim 0.64$ of hard spheres is well defined [6] although its precise value is unknown. On the other hand, Torquato *et al.* [7] argued that $\phi_{\rm rcp}$ is ill defined as the jamming density depends strongly on the compression rate. These authors showed by simulations of pure hard spheres and binary hard-disk mixtures that the jamming density increases with slower compressions due to crystallization (and demixing) [7,8]. They resolved this issue by defining a maximally random jammed state which only takes into account systems that do not have any crystalline order and find that the equation of state (EOS) of the metastable fluid diverges at $\phi_{\rm rcp} \sim 0.644$ [9].

Crystallization can be avoided by introducing size polydispersity. In this letter, we study the jamming density as a function of compression rate for polydisperse colloidal hard spheres. We find that the jamming density increases by lowering the compression speed without introducing any *crystalline order* into the system in contrast with previous results [7,8]. Moreover, our results contrasts the idea that $\phi_{\rm rcp}$ is well defined and can be regarded as the infinite-pressure limit of the metastable extension of the equilibrium liquid branch [6,7,9].

Others made the assumption that jammed configurations can be regarded as the infinite-pressure limit of glassy states [10–13]. Speedy [11] showed that different hard-sphere glasses can be generated with different jamming densities due to irreversible relaxation. Recent simulations on binary hard-sphere mixtures also confirm this assumption [14,15]. To investigate whether our observed range of jamming densities can be explained by the idea that different glasses jam at different

densities, we monitor the pressure during compression. Our results provide evidence that jammed configurations of polydisperse hard spheres can be regarded as the infinite-pressure limit of glassy states and that indeed different glasses can be formed for different compression rates that jam at varying jamming densities.

Additionally, we give accurate data for the jamming density as a function of compression rate and size polydispersity, which is important for experiments on colloidal systems, where the packing fraction is often determined by equating the packing fraction of the centrifuged sediment to $\phi_{\rm rcp}$ obtained from simulations [16,17]. However, it was already pointed out in [18] that these simulation results are inaccurate, thereby casting doubts on the determination of the volume fractions in these experiments [5]. Additionally, these simulations do not take any compression rate (or centrifugal speed) dependence into account. As our results show that the jamming density strongly depends on the compression rate, we denote the density of the jammed configuration with ϕ_J rather than the random-close-packing density $\phi_{\rm rcp}$. We also note that jammed configurations are defined here as infinite-pressure states as further compression would result in particle overlaps; it does not mean that particles cannot displace anymore or cannot move collectively.

As the focus of our work is on colloidal hard spheres with a well-defined temperature, and where the particles cannot be deformed or overlap, we restrict ourselves to simulations that strictly prohibits particle overlaps. In addition, we kept the temperature and hence, the kinetic energy of all particles fixed. This is an important difference with the work on soft particles [19–21]. To this end, we perform event-driven molecular-dynamics (MD) simulations using the Lubachevsky-Stillinger algorithm [22]. Modifications were made to fix the temperature of the system and to define a compression rate $\Gamma = {\rm d}\sigma V^{-1/3}/{\rm d}t$, where we use the MD time as our unit of time [23]. The temperature was kept constant by monitoring the build up of kinetic energy and by rescaling the particle velocities. When we rescaled the velocities we also rescaled the system size such that the average diameter of the particles was kept fixed. So the algorithm runs for a certain number of collisions while the temperature rises and the particles grow. The algorithm was adapted to keep the polydispersity constant during the particle growth [24]. When the temperature of the system rises too much or the particles become too large, the system is rescaled to the desired temperature and particle sizes. The polydispersity was sampled from a log-normal distribution, which is nearly identical to a normal (Gaussian) distribution for small polydispersities, but has the advantage that it is zero for negative diameters.

We determine the EOS from simulations of 2000 particles with a size polydispersity of 10%. We average our results over 50 different runs. To check for finite-size effects we perform simulations with up to 2 $\times 10^5$ particles and we find good agreement within the statistical accuracy. We plot the EOS for varying Γ in fig. 1a along with the

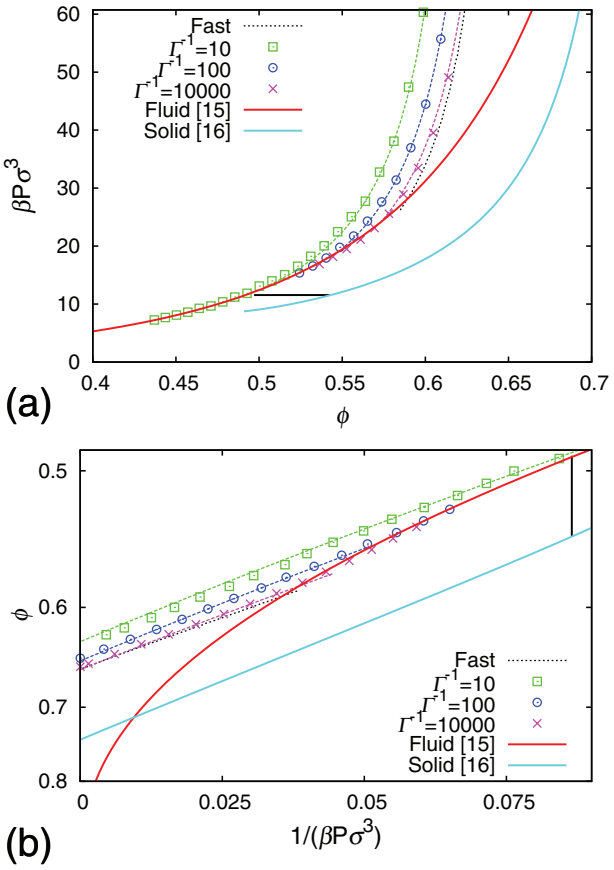

Fig. 1: (Colour on-line) (a) Pressure $\beta P\sigma^3$ as a function of packing fraction ϕ for a system of hard spheres with 10% size polydispersity and for varying compression rates Γ as labeled. The dotted black line is a fast compression of a well-equilibrated fluid of $\phi = 0.585$. The red and blue (dark and light solid) lines denote the equilibrium equation of state for the fluid and solid phase, respectively, while the horizontal line denotes fluid-solid coexistence. The dashed lines denote the fits to the simulation data (symbols) using eq. (1). (b) As in (a) but now plotted as a function of ϕ and $1/(\beta P\sigma^3)$ so that the infinite-pressure limit is clearly visible.

equilibrium Carnahan-Starling (CS) EOS for the fluid [25] and the EOS of the solid phase [11]. During the simulations with 10% polydispersity, we carefully checked for crystallization, but we did not find any crystalline order in any of our compression runs. The global bond-orientational order parameter Q_6 remains <0.02 during compression for all Γ, and the pressure does not show any drops that correspond with partial crystallization. We also calculated local and global Q_4, Q_6 and Q_8 bond-orientational order parameters, which did not show any local and global crystalline order. Additionally, the spatial correlation function of Q_6 [26] did not detect any crystalline clusters. We also checked for demixing by calculating the number of particles that are smaller or larger than the averaged size around each particle during the simulation. As this number remains constant, we conclude that we did not find any sign of demixing.

The pressure initially follows the equilibrium CS-EOS of the metastable fluid phase until the system becomes kinetically arrested as the relaxation time of the system exceeds the compression rate. At this density, the pressure increases much faster than that of the equilibrium fluid EOS upon further compression. The density of the jammed configuration at infinite pressure increases with slower compressions. The reason is that the system has more time to equilibrate for slow compressions, and hence the system falls out of equilibrium at a higher density on the metastable fluid branch. Further compression of this glass phase yields a higher jamming density. Therefore we find a finite range of jamming densities depending on Γ. Our results provide strong support that jammed configurations can be identified with the infinite-pressure limit of glassy states and that different glasses can be generated as a function of compression rate that jam at different densities.

We note that fig. 1a shows remarkable resemblance to fig. 7 of [15], where the existence of multiple EOS for the unequilibrated binary hard-sphere glasses has been established, all diverging at different jamming densities. In addition, they construct a one-to-one correspondence between the density where the system falls out-of-equilibrium and the density where the pressure diverges by equilibrating metastable fluid configurations at various initial densities and compressing them rapidly to very high pressures so that structural relaxation is prevented. In this work, we keep the compression rate fixed during the compressions as this is closer to the experimental conditions of colloidal systems. Appreciable relaxation and aging behaviour might be expected during our compressions when the system departs the equilibrium EOS. However, we do not find any noticeable effect on the jamming density if we increase the compression rate when the system leaves the equilibrium liquid branch.

The concept of multiple glasses is well known for molecular glasses [27]. Indeed, fig. 1a resembles the picture that is found for molecular glasses with ϕ and $1/(\beta P\sigma^3)$ playing the role of the inverse of the specific volume and the temperature, respectively. To this end, we plot our results in fig. 1b in the ϕ-$1/(\beta P\sigma^3)$ representation, where $\beta = 1/k_BT$ with k_B Boltzmann's constant. We now find striking similarities with the sketched phase diagrams in refs. [12,13]. Theoretical calculations using the replica method [13] predict also that different glasses can jam at different densities upon compression, and that the pressure of the glass phase close to jamming is well described by a power law $\beta P/\rho \propto 1/(\phi_J - \phi)$ with ϕ_J the jamming density at infinite pressure [13]. We observe in fig. 1b an almost linear behavior for the inverse pressure as a function of ϕ for the glass phase, which we can fit remarkably well as shown in fig. 1 over the full range using the free volume scaling [6]:

$$\beta P\sigma^3 = a\frac{\phi_J^{1/3}\phi^{2/3}}{(\phi_J/\phi)^{1/3}-1}, \qquad (1)$$

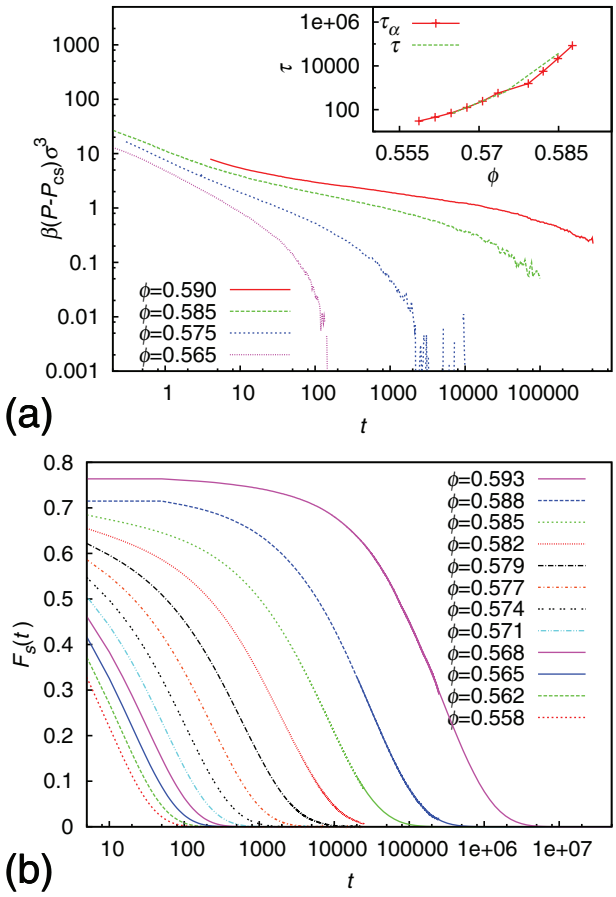

Fig. 2: (Colour on-line) (a) Pressure difference $\beta(P(t) - P_{CS})\sigma^3$ with respect to the Carnahan-Starling equation of state P_{CS} as a function of MD time for a system of hard spheres with 10% size polydispersity. Inset: the relaxation time τ_α and τ of the self-intermediate scattering function $F_s(t)$ and $P(t)$, respectively. (b) $F_s(t)$ as a function of MD time.

where a and ϕ_J are fitting parameters. The leading order term of eq. (1) yields the power law as predicted in [13] close to jamming. In addition, the theory predicts an ideal-glass transition at a Kauzmann packing fraction $\phi_K = 0.617$ on the metastable fluid branch, yielding a jammed configuration upon compression of this ideal glass with a random-close-packing density of $\phi_{\rm rcp} = 0.683$ [13]. However, the existence of a thermodynamic ideal-glass transition is heavily debated. We note that our results do not depend on the (non-)existence of such a glass transition. Our results show a nonequilibrium glass transition at a density range of 0.50–0.59, which is far below the theoretical predictions for the ideal glass. This is to be expected as the structural relaxation time diverges on approaching the ideal-glass transition [28]. Hence, it is impossible to reach ϕ_K, since already at lower densities, the fluid gets arrested in a nonequilibrium glass as the relaxation time becomes longer than the simulation time.

In order to investigate the divergence of the structural relaxation time on approaching ϕ_K, and to estimate what the maximum density is at which we can still equilibrate a state on the metastable fluid branch, we

perform constant-volume simulations of a system of 2×10^4 spheres with 10% size polydispersity and varying ϕ. We start our runs with an initial configuration obtained from a fast compression. Figure 2 shows the pressure difference with respect to the CS-EOS as a function of time. We clearly observe that the pressure initially decays towards an intermediate state for all ϕ. Subsequently, large collective rearrangements are required to relax the system further. Finally, we observe that the pressure reaches the value predicted by the equilibrium CS-EOS. The time scale for the system to equilibrate to the equilibrium fluid phase is comparable to the relaxation time τ_α that can be determined from the self-part of the intermediate scattering function $F_s(q,t)$, where we define τ_α by $F_s(\tau_\alpha) = 0.1$ for $q\sigma = 6.5$. In fig. 2b we plot $F_s(t)$ for varying ϕ and the inset of fig. 2a shows τ_α along with the equilibration time τ defined as $\beta(P(\tau) - P_{CS})\sigma^3 = 0.1$. We clearly observe that both times are remarkably close. The equilibration time of a system with 2×10^4 particles at $\phi = 0.585$ is more than 10^5 MD steps, which is equivalent to 2 weeks on a desktop PC. The equilibration time for $\phi = 0.59$ is expected to be more than 20 weeks. Hence, the ideal glass at ϕ_K, and the corresponding random close packing are both inaccessible. Instead the system will fall out of equilibrium into a non-equilibrium glass state at a density that depends strongly on the compression rate. Additionally, we compress at high Γ our well-equilibrated fluid configuration of $\phi = 0.585$ to very high pressures as in [15]. Figure 1 shows that the EOS is similar to the other compression runs, providing again support that jammed configurations are infinite-pressure limits of glassy states.

In order to study whether the final configurations are locally or collectively jammed, we calculate the coordination number of the final configuration of the monodisperse compression runs. To calculate the coordination number we perform a short event driven MD simulation, initialized with the final configuration of the compression run, while we keep track of the collisions of all particles. In fig. 3a we plot the averaged number of neighboring particles with which each particle has collided as a function of time. For very fast compressions, the particles can still move out of their cage and collide with new particles, while for slower compressions, the cage formed by on average 6 neighbors gets tighter. Hence, it takes longer till a particle can escape out of its cage and collide with more than 6 particles. The slowest compressions result in a nearly rectangular graph where the particles can only collide with the 6 particles of its cage. As the averaged coordination number is always larger than 4 and the cage-trapping plateau of the mean square displacement is always much smaller than σ^2, we conclude that the configurations are at least locally jammed [29].

However, for all compression speeds the particles are still able to escape their cages by collective rearrangements, although this takes longer for slower compressions. We can read of the number of particles that have escaped their cage from fig. 3, when we assume that particles are

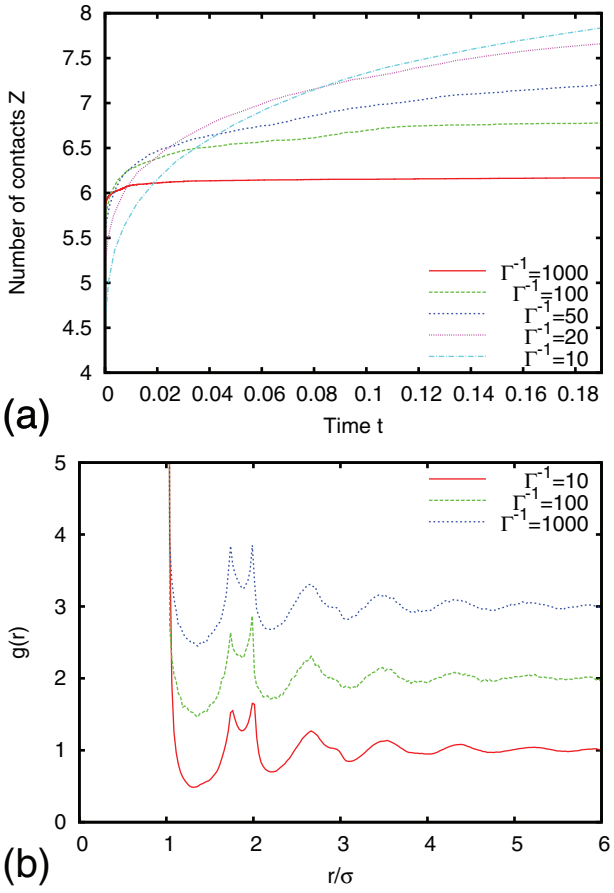

Fig. 3: (Colour on-line) (a) The coordination number obtained from the number of different particles a particle has collided with after time t in MD units. The simulations were started with the final configuration of a monodisperse compression run. (b) The radial distribution functions of the final configurations of the monodisperse compression runs for varying Γ^{-1} as labeled.

caged by maximally 6 neighbors and all particles that have collided with a 7th particle have escaped their cage. The fact that we do not observe collectively jammed configurations is consistent with work of Donev *et al.* [30] who have demonstrated that it is difficult to generate large collectively jammed systems and Osada [31] and Salsburg *et al.* [32], who have proven that it is impossible to have an infinitely large collectively jammed system of Brownian particles at finite pressure. Our system contains 2000 particles which is most likely too large to result in a collectively jammed configuration at the pressures we have reached.

Our results differ significantly from studies on collectively jammed configurations of soft particles at temperature $T = 0$, where a well-defined jamming point or random-close-packing density is found in the thermodynamic limit [19,20]. In these studies, although they might yield overlap-free final configurations, will follow a path through phase space that cannot be followed by hard particles without generating particle overlaps. Recent work shows, however, that these soft-particle systems yield a range

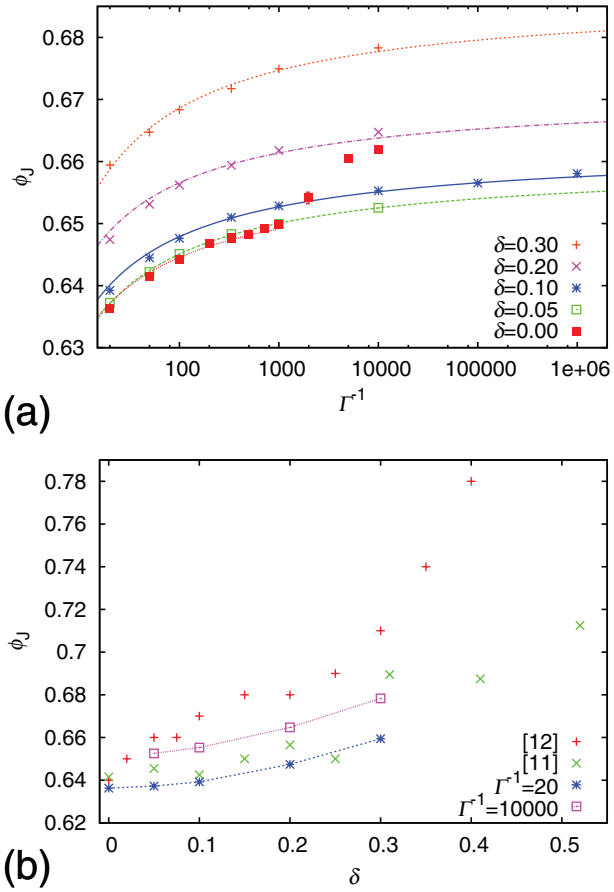

Fig. 4: (Colour on-line) (a) Jamming density ϕ_J as a function of the inverse compression rate Γ^{-1} for polydispersities δ as labeled. The lines denote fits to our results (see text). (b) ϕ_J *vs.* δ for $\Gamma^{-1} = 20$ and 10^4. Data from [16,17] are denoted by crosses and plusses.

of jamming densities as the compression is performed at finite temperature [21].

To investigate whether there is a structural difference between the different compression speeds we calculated the radial distribution function of the monodisperse final configurations in fig 3b. The radial distribution functions of these different configurations are nearly independent of the compression speed and show all the typical features observed for dense random packings of spheres, *i.e.*, split second peak, oscillatory decay, averaged coordination number larger than 4, etc. [33].

Finally, we study the jamming density as a function of Γ for several size polydispersities δ. We perform simulations of 2000 particles using varying Γ and we terminate the simulations when the time between successive collisions becomes of the same order of magnitude as our numerical accuracy, yielding $\beta P\sigma^3 \sim 10^5$ for slow compressions. To determine the jamming density ϕ_J, we fit the EOS close to jamming (the last few volume percent) with eq. (1). We average our results over 50 different runs. Figure 4a shows ϕ_J as a function of Γ^{-1} for varying δ. We have fitted these extrapolations with $\phi = a + b/\log(\Gamma)$, where a and b are fitting parameters. The jamming density ϕ_J for pure hard spheres ranges from 0.635 to 0.645 for $10 \leqslant \Gamma^{-1} \leqslant 1000$. For faster compressions $\Gamma^{-1} < 10$, the simulations do not yield jammed configurations and the system (partially) crystallizes for $\Gamma^{-1} > 1000$ as can be observed in fig. 4 as ϕ_J increases rapidly, which is consistent with [7]. We also observe that ϕ_J increases with increasing δ. For $\delta = 10\%$, we find that ϕ_J varies from $0.638 - 0.658$. As polydispersity prevents crystallization, we are now able to study ϕ_J for five orders of magnitude of Γ. Although the slope of the curves decreases with increasing Γ^{-1} (slower compressions), it is hard to justify an extrapolation to infinitely slow compression rates. Figure 4b shows ϕ_J as a function of δ for $\Gamma^{-1} = 20$ and 10^4. For comparison, we also plot data from Nolan [16] and Schaertl [17]. Our results are close to [16], but the results of [17], which are obtained from single runs with low accuracy, deviate from our data. The strong Γ-dependence of ϕ_J explains the range of densities that has been found in the literature obtained by different authors and algorithms. Our results show that a size polydispersity of up to 5% does not increase the jamming density significantly from the monodisperse case. A much larger dependence on δ is often used in the experiments [5] based on ref. [17], casting doubts on the precise values for the volume fractions determined in experiments via this route.

In conclusion, we studied the jamming density of colloidal hard spheres as a function of compression rate for a wide range of size polydispersities. As the focus of our work is on jamming in systems of colloidal hard spheres with a well-defined temperature, we employed event-driven MD simulations at finite temperature (fixed kinetic energy) using an algorithm that strictly prohibits particle overlaps. We find a range of jamming densities as a function of compression rate. We show that the increase in jamming density cannot be explained by crystallization effects in contrast with [7]. In addition, our results contrasts the idea that the jamming or random-close-packing density $\phi_{\rm rcp}$ is well defined and can be regarded as the infinite-pressure limit of the metastable liquid branch [6,7,9]. Instead we find that jammed configurations of polydisperse hard spheres can be identified as the infinite-pressure limit of glassy states and that different glasses can be formed that jam at different jamming densities as a function of the compression rate. Our work demonstrates nicely the compression rate dependence of ϕ_J for a wide range of size polydispersities and complement recent work that showed the existence of multiple glassy states and jamming densities for binary mixtures of hard spheres [14,15].

* * *

We thank L. Berthier and S. Torquato for useful comments and discussions.

REFERENCES

[1] Hales T., *Ann. Math.*, **162** (2005) 1065.
[2] Pusey P. N. and van Megen W., *Nature*, **320** (1986) 340.
[3] van Blaaderen A. and Wiltzius P., *Science*, **270** (1995) 1177.
[4] Liu A. and Nagel S., *Nature*, **396** (1998) 21.
[5] Ballesta P. *et al.*, *Phys. Rev. Lett.*, **101** (2008) 258301; Dullens R. P. A. *et al.*, *Phys. Rev. Lett.*, **97** (2006) 228301; Petekidis G. *et al.*, *Phys. Rev. E*, **66** (2002) 51402; Kegel W. and van Blaaderen A., *Science*, **287** (2000) 290.
[6] Kamien R. D. and Liu A. J., *Phys. Rev. Lett.*, **99** (2007) 155501.
[7] Torquato S. *et al.*, *Phys. Rev. Lett.*, **84** (2000) 2064.
[8] Donev A. *et al.*, *Phys. Rev. Lett.*, **96** (2006) 225502.
[9] Rintoul M. D. and Torquato S., *Phys. Rev. Lett.*, **77** (1996) 4198.
[10] Woodcock L. V. and Angell C. A., *Phys. Rev. Lett.*, **47** (1981) 1129.
[11] Speedy R. J., *Mol. Phys.*, **95** (1998) 169.
[12] Mari R. *et al.*, *Phys. Rev. Lett.*, **103** (2009) 025701.
[13] Parisi G. and Zamponi F., arXiv:0802.2180 (2008).
[14] Biazzo I., Caltagirone F., Parisi G. and Zamponi F., *Phys. Rev. Lett.*, **102** (2009) 195701.
[15] Berthier L. and Witten T. A., *Phys. Rev. E*, **80** (2009) 021502.
[16] Nolan G. and Kavanagh P., *Powder Technol.*, **72** (1992) 149.
[17] Schaertl W. and Sillescu H., *J. Stat. Phys.*, **77** (1994) 1007.
[18] El Masri D. *et al.*, *J. Stat. Mech.* (2009) P07015.
[19] Xu N. *et al.*, *Phys. Rev. E*, **71** (2005) 061306.
[20] O'Hern C. S. *et al.*, *Phys. Rev. E*, **68** (2003) 011306.
[21] Chaudhuri P., Berthier L. and Sastry S., arXiv:0910:0364 (2009).
[22] Lubachevsky B. D. and Stillinger F. H., *J. Stat. Phys.*, **60** (1990) 561.
[23] Speedy R. J., *J. Chem. Phys.*, **100** (1994) 6684.
[24] Kansal A. *et al.*, *J. Chem. Phys.*, **117** (2002) 8212.
[25] Carnahan N. F. and Starling K. E., *J. Chem. Phys.*, **51** (1969) 635.
[26] ter Wolde P. R., Ruiz-Montero M. J. and Frenkel D., *Phys. Rev. Lett.*, **75** (1995) 2714.
[27] Kauzmann W., *Chem. Rev.*, **43** (1948) 219.
[28] Brambilla G. *et al.*, *Phys. Rev. Lett.*, **102** (2009) 085703.
[29] Torquato S. and Stillinger F. H., *J. Phys. Chem. B*, **105** (2001) 11849.
[30] Donev A., Torquato S. and Stillinger F. H., *Phys. Rev. E*, **71** (2005) 011105.
[31] Osada H., *Probab. Theory Relat. Fields*, **112** (1998) 53.
[32] Salsburg Z. W. and Wood W. W., *J. Chem. Phys.*, **37** (1962) 798.
[33] Torquato S. and Stillinger F. H., *J. Phys. Chem. B*, **106** (2002) 8354.